

# Parametric Study for Lateral Jet Interaction in Supersonic Flow

Yoon Woo Lee\*, Yung Hwan Byun, Soo Hyung Park\*\* and Jong Kook Lee\*\*\*

\*Graduate School of Aerospace Information Engineering, Konkuk University  
Seoul, Republic of Korea

\*\*Department of Aerospace Information Engineering, Konkuk University  
Seoul, Republic of Korea

\*\*\*Wind Tunnel Laboratory, Agency for Defense Development  
Daejeon, Republic of Korea

## Abstract

An experimental and computational study on the supersonic flow around the lateral jet has been performed. The present experimental study on the lateral jet interaction was carried out in Konkuk University's supersonic wind tunnel MAF. The experimental techniques include Schlieren visualization and pressure sensor. Three-dimensional RANS computations were done and compared with the experimental data. The physical phenomena on the jet interaction were investigated with lateral jet Mach number, specific heat ratio and pressure ratio. A parametric study shows that the variation of the pitching moment is largely affected by both lateral jet Mach number and pressure ratio.

## 1. Introduction

Conventional missile attitude controls (Tail, Canard, Wing, and TVC) are shown in left side of a Figure 1. There are limitations in a response time and mobility to use of a conventional missile control due to a control surface reaction. Effective maneuver is difficult because dynamic pressure is very low at a high altitude and a low speed. Because of the previous shortcomings, there is focused attention to an unconventional missile attitude control like the lateral jet attitude control.

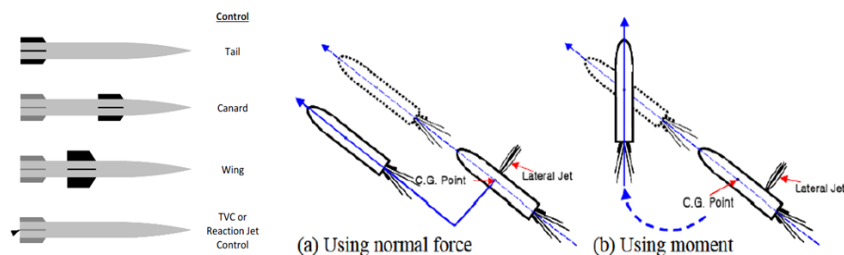


Figure 1: Conventional and Lateral Jet Attitude Control on Missile [1]

The lateral jet controls are shown in right side of Figure 1. The lateral jet can be used in two ways as an attitude control. It can be located at the center of gravity and a controlling translation. Placing the jet away from the center of gravity makes pitch or yaw moment. The lateral jet can have a higher response time and mobility than the conventional control at high altitude and low speed. However, lateral jet has a few disadvantages. The lateral jet has a complex three-dimensional flow by an interaction with freestream and lateral jet. And lateral jet has complex structure for taking propellant, installing the combustion chamber and nozzle at the required operating position. An actively research is needed because of a higher efficiency than in the conventional control. [1, 2, 3]

The lateral jet structure is shown in Figure 2. The lateral jet acts as a virtual obstacle to free stream. This obstacle causes a bow shock to upstream of the lateral jet. The pressure gradient across the bow shock induces separation of the boundary layer, which it creates a separation shock. A pair of counter rotating vortices is created in the downstream region due to mixing of free stream and the lateral jet. Moment occurs because upstream of jet is high pressure region and downstream region is low pressure region. [3]

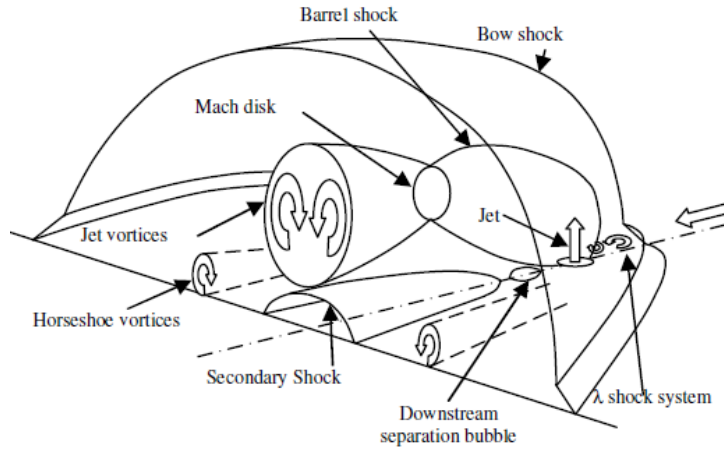


Figure 2: Interaction with the lateral jet and free stream [4]

The purpose of this investigation is parametric study according to variation of the lateral jet Mach number, pressure ratio, and specific heat ratio. Schlieren visualization and pressure measurement are conducted about the lateral jet at Konkuk University's supersonic wind tunnel. And computational fluid analysis is performed using the FLUENT to compare experiment.

## 2. Experimental Setup and Instrumentation

### 2.1 Test Model and Wind Tunnel Facility

The test model used for these investigations is a flat plate. It consists of a flat plate and two kind of the lateral jet nozzle. Flat plate has 50mm in span and 5mm in thickness for ensured that no choking of the tunnel occurs with the given dimensions of the test model. Mach number 1 and 3.7 lateral jet nozzles are located on the midsection at flat plate. Its axis is normal to the model axis. A circular lateral jet nozzle of 2mm in throat diameter is made for same mass flow rate. Mach number 3.7 nozzle has 15 degree divergent angle and 45 degree convergent angle. Test model has 1mm in diameter and 10 pressure tabs for measure surface pressure.

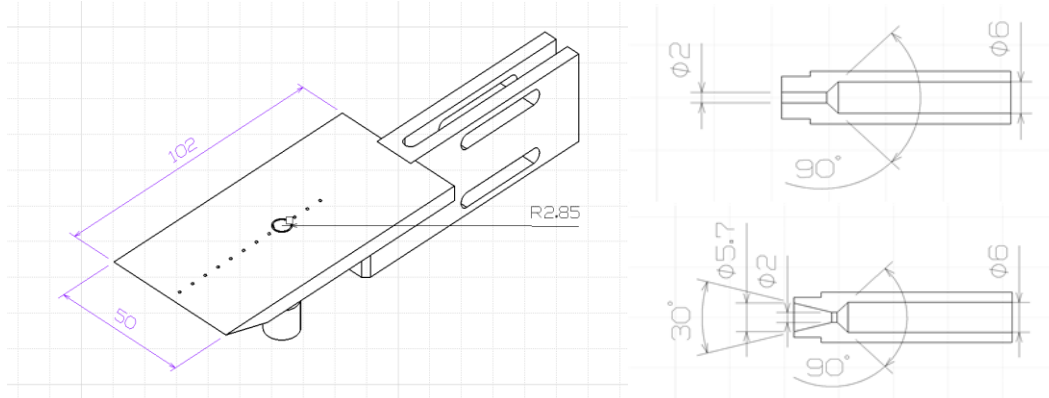


Figure 3: Flat Plate and Lateral Jet Model

The experiments are conducted in the supersonic wind tunnel MAF(Model Aerodynamic Facility) of Konkuk University at a Mach number of 3. This facility operates in the blow-down mode with blow duration of typically 2 sec. The Reynolds number is  $3.83 \times 10^6$ . The static wind-tunnel free-stream pressure is  $P_\infty = 2.387 \times 10^5 \text{ Pa}$ . The test model is mounted on a sing assembly along the tunnel centerline.

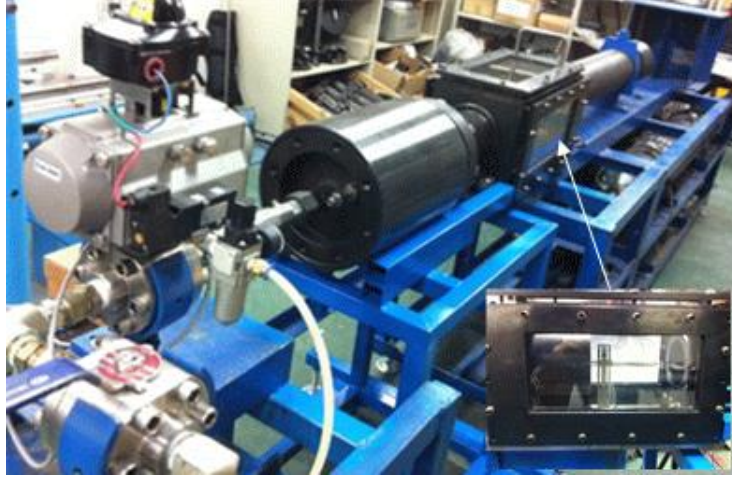


Figure 4: MAF (Model Aerodynamic Facility)

## 2.2 Flow Visualization Technique

Schlieren flow visualization is based on the deflection of light by refractive index gradient. Schlieren visualization is made using an 80 W LED light source, a 12-bit CCD camera (Model PCO 1600). This camera is used in the  $2 \times 2$  binning mode, resulting in an effective resolution of  $800 \times 600$  pixels and the exposure time is  $50 \mu\text{s}$ .

## 2.3 Pressure Measurement System

A static pressure measurement of the surface pressure on the model is carried out with the aid of a Netscanner 9116 pressure scanning and data acquisition system from Pressure Systems Inc. (PSI). Netscanner 9116 is including 16 channels and measuring range is 45 psi. Data acquisition system is NUSS (Netscanner Unified Startup Software). The error on the static pressure is lower than  $\pm 0.05\text{FS}$ .

## 3. Numerical Simulations

The numerical simulations of the interaction of the lateral jet flow with the external flow are conducted by means of FLUENT. The flow field surrounding a lateral jet in external flow is highly complex. Many different turbulence model was have been used to simulate the jet interaction. Turbulence model used for this investigation is  $k-\omega$  SST and 2<sup>nd</sup> order AUSM method is used. And ideal gas and steady state are assumed.

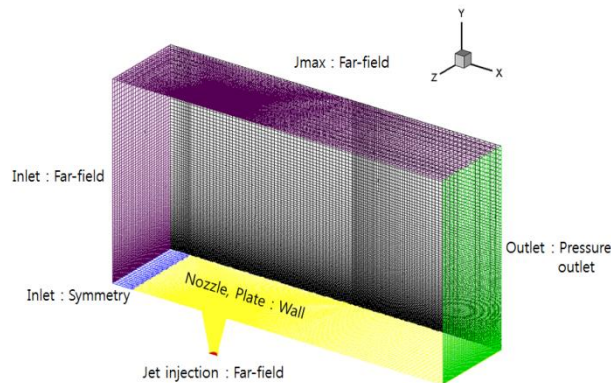


Figure 5: Computational Domain and Boundary Conditions

Figure 5 show the three-dimensional grid and boundary conditions. Computational domain is reduced to 1/2 of the complete domain because the symmetry of the problem. Near the lateral jet outlet, grid is concentrated due to sharply change of property. Grid has  $2 \times 10^6$  structured cells and size is same based on experimental model. Figure 6 show the compare  $M_j = 1.0$  and  $M_j = 3.7$  grid. Each has same throat diameter and  $M_j=3.7$  has 45 degree divergent angle based on experimental model.

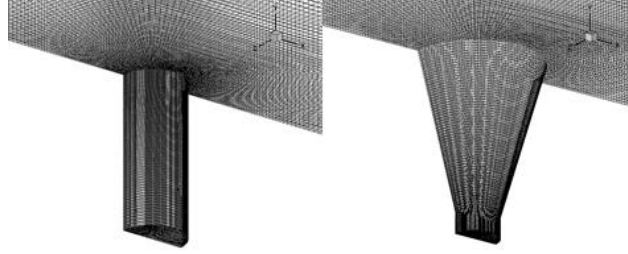


Figure 6:  $M_j=1.0$ ,  $M_j=3.7$  Nozzle Grids

#### 4. Results and Discussion

Experiments are conducted with variation of injection Mach number ( $M_j$ ), Pressure Ratio (PR), Specific heat ratio ( $\gamma$ ). PR is defined by the following expression.

$$PR = \frac{P_{0j}}{P_\infty} \quad (1)$$

PR notation is used at injection Mach number and PR studies. However, Momentum Parameter Ratio (MPR) is needed at specific heat ratio study. MPR is defined by the following expression.

$$MPR = \frac{(\gamma PM^2)_j}{(\gamma PM^2)_\infty} \quad (2)$$

Experimental and CFD conditions are shown at Table 1.

Table 2: Experimental and CFD conditions

	Parameter	Fixed value	Experiment	CFD
4.1	$M_j$	PR = 200 Gas = Air	1.0	1.0
			x	1.5
			x	2.0
			x	2.5
			x	3.0
			3.7	3.7
4.2	PR	$M_j=3.7$ Gas = Air	40	
			80	
			120	
			160	
			200	
4.3	$\gamma$	$M_j=3.7$ MPR = 0.5, 1.0, 1.5, 2.0, 2.5	Air	x
			Carbon dioxide	x
			Helium	x

##### 4.1 Effects of Injection Mach number

Schlieren and numerical schlieren image of  $M_j=1.0$ , 3.7 are shown in Figure 7. Schlieren and numerical schlieren image has similar structure (Separation shock, Bow shock, and Barrel shock) in each case. Separation bubble at  $M_j=1.0$  is larger than  $M_j=3.7$ . Separation bubble size depends on adverse pressure gradient. Nozzle exit static

pressure at  $M_j=1.0$  is 2,113,120 Pa and at  $M_j=3.7$  is 39,600 Pa. Thus separation bubble at  $M_j=1.0$  is larger than  $M_j=3.7$ .

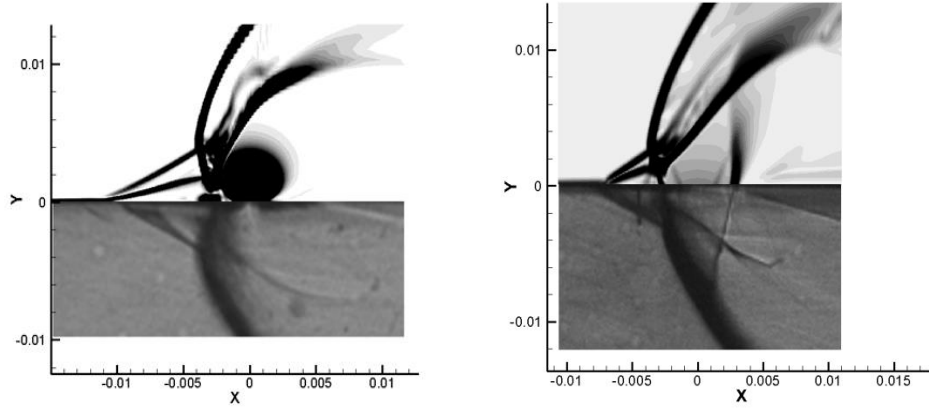


Figure 7: Schlieren (Lower) and Numerical schlieren (Upper) image (Left:  $M_j=1.0$ , Right:  $M_j=3.7$ )

Qualitative information such as the flow structure was obtained using schlieren and numerical schlieren visualization. Quantitative information such as the pitching moment coefficient was obtained using surface pressure measurement. Moment center is lateral jet nozzle center. Pitching moment coefficient equation is defined by the following expression. Pitching moment coefficient is calculated by using CFD result.

$$C_m = \frac{1}{c^2} [\int (C_{p,u} * x) dx] \quad (3)$$

Pitching moment coefficient at  $M_j=1.0$  is -0.02165 and  $M_j=3.7$  is -0.01431. It seems pitching moment is reduced by increasing of  $M_j$ . CFD works of  $M_j=1.5, 2.0, 2.5, 3.0$  are performed to see moment variation according to detail variation of  $M_j$ . Jet thrust force by the lateral jet is shown at Table 3. As increasing of  $M_j$ , jet thrust force is also increasing. Pitching moment coefficient variation according to  $M_j$  is shown at Figure 8. As shown in Figure 8, Pitching moment coefficient has maximum value at  $M_j=1.5$  and coefficient is decrease after that value.

Table 3:  $F_j$  vs  $M_j$

$M_j$	1.0	1.5	2.0	2.5	3.0	3.7
$F_j(N)$	15.86	16.62	17.76	18.72	19.41	19.84

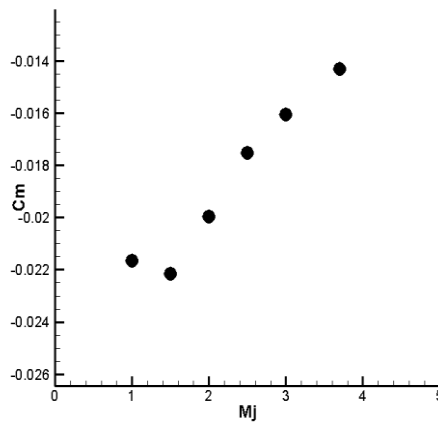


Figure 8:  $C_m$  vs  $M_j$

## 4.2 Effects of Pressure Ratio

Schlieren images of  $PR=40, 80, 120, 160, 200$  are shown in Figure 9. The lateral jet gas is Air and freestream Mach number is 3. Separation region is increases according to increase of  $PR$ . And barrel shock and bow shock gradient are also increase according to increase of  $PR$ .

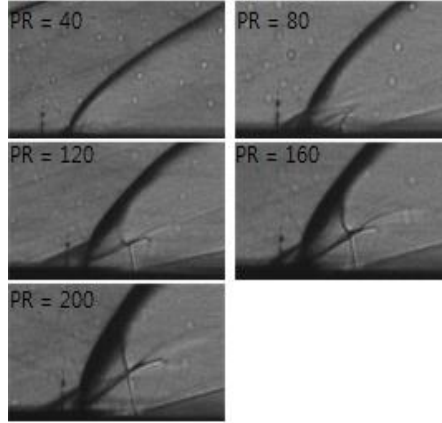


Figure 9: Schlieren images of variation of  $PR$

Pitching moment coefficient variation according to  $PR$  is shown at Figure 10. As shown in Figure 10, Pitching moment coefficient is gradually increase to  $PR = 160$ . However, there is no increasing after  $PR=160$ .

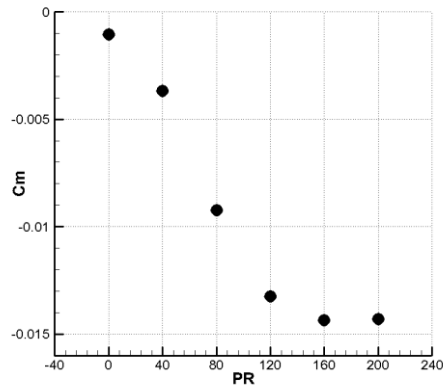
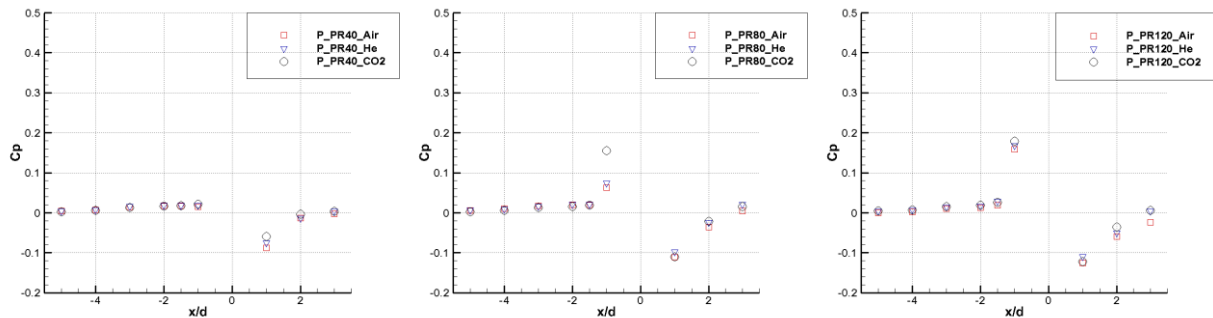
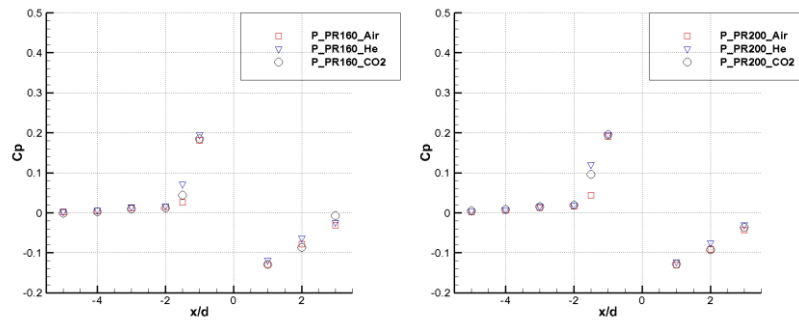


Figure 10:  $C_m$  vs  $PR$

## 4.3 Effects of Injection gas

Pressure coefficients of injection gases Air, CO<sub>2</sub>, Helium in  $PR = 40, 80, 120, 160, 200$  are shown in Figure 11. Pressure coefficients are made by surface pressure measurement. As shown at Figure 11, there are no significant differences between injection gases.



Figure 11:  $C_p$  vs Lateral jet injection gas

## 5. Conclusion

The purpose of this investigation is parametric study according to variation of the lateral jet Mach number, pressure ratio, and specific heat ratio. The experiments are conducted in the supersonic wind tunnel MAF. And computational fluid analysis is performed using the FLUENT to compare experiment. With variation of the lateral jet Mach number, there are some differences on flow structure and it cause difference of pitching moment coefficient. Pitching moment coefficient has maximum value at  $M_j=1.5$  and coefficient is decrease after that value. With variation of pressure ratio, also has difference on flow structure. Pitching moment coefficient is gradually increase to  $PR = 160$ . However, there is no increasing after  $PR=160$ . With variation of injection gas, there are no significant difference between injection gases. Actually the real lateral jet uses burned hot gases it has 3000K and diffent specific heat ratio. Thus the continuous reasearch about variation of specific heat ratio is required.

## Acknowledgement

This research was supported by the Space Core Technology Development Program through the National Research Foundation of Korea funded by the Ministry of Science, ICT and Future Planning(No:20110020837)

## References

- [1] Min, B. Y, Lee, J.W, Byun, Y. H. Hyun, J. S. 2002. A study of supersonic flow around lateral jet controlled missile. *Korea Society for Computational Fluids Engineering*.
- [2] Min, B. Y, Lee, J.W, Byun, Y. H. Hyun, J. S, Kim, S. H. 2004. Numerical Investigation of the lateral jet effect on the aerodynamic characteristics of the missile. *The Korean Society for Aeronautical and Space Sciences*. 64 - 71.
- [3] Christie, R. 2010. Lateral jet interaction with a supersonic crossflow. MSc Thesis. Cranfield University, School of engineering.
- [4] Dean A. Dickmann, Frank K. Lu, 2008, Shock/Boundary layer interaction effects on transverse jets in crossflow over a flat plate. In: 38<sup>th</sup> AIAA Fluid Dynamics Conference and Exhibit.
- [5] Gnemmi, Patrick, and Hans-J. Schafer. 2005, Experimental and numerical investigations of a transverse jet interaction on a missile body. In: 43th AIAA Aerospace Sciences Meeting and Exhibit.
- [6] Palekar, Amol, C. Randall Truman, and Peter Vorobieff. 2005. Prediction of transverse injection of a sonic jet in supersonic crossflow. 36th AIAA plasmadynamics on lasers conference.
- [7] Papamoschou, Dv, and D. G. Hubbard. 1993. Visual observations of supersonic transverse jets. *Experiments in Fluids*, 14(6).
- [8] Seiler, F., Gnemmi, P., Ende, H., Schwenzer, M., & Meuer, R. 2003. Jet interaction at supersonic cross flow conditions. *Shock Waves*, 13(1).
- [9] Aswin, G., and Debasis Chakraborty. 2010. Numerical simulation of transverse side jet interaction with supersonic free stream. *Aerospace Science and Technology* 14(5),
- [10] Gruber, M. R., et al. 1995. Mixing and penetration studies of sonic jets in a Mach 2 freestream. *Journal of Propulsion and Power*, 11(2).
- [11] Stahl, B., H. Esch, and A. Gülhan. 2008. Experimental investigation of side jet interaction with a supersonic cross flow. *Aerospace Science and Technology*, 12(4).